

# The Impact of Numerology on the PDSCH Throughput of the 5G Downlink

**Abdullah Alsir Mohamed**

Department of Computer Engineering, College of Computer Engineering and Sciences, Prince Sattam bin Abdulaziz University, Al-Kharj, 11942, Saudi Arabia  
a.mhamed@psau.edu.sa (corresponding author)

Received: 11 July 2024 | Revised: 4 August 2024 | Accepted: 11 August 2024

Licensed under a CC-BY 4.0 license | Copyright (c) by the authors | DOI: <https://doi.org/10.48084/etasr.8370>

## ABSTRACT

The introduction of 5G technology has provided numerous improvements in wireless communication systems, like higher data rates, lower latency, power efficiency, and enhanced spectral efficiency. Subcarrier spacing is one of the most important elements affecting system performance. This paper studies the influence of numerology on the Physical Downlink Shared Channel (PDSCH) throughput in the 5G NR downlink. Two types of channel models and different bandwidths are used to evaluate the throughput as a function of the signal-to-noise ratio. This paper aims to find the right numerology for various bandwidths, channel models, and signal-to-noise ratio levels. Results show that the throughput increases as the numerology index decreases for the CDL-C channel model. In contrast, for the TDL-C channel model, increasing the numerology index does not always mean increasing throughput. It can result in decreased throughput in some scenarios.

*Keywords- numerology; 5G; throughput; CDL-C; TDL-C*

## I. INTRODUCTION

Multiple numerologies in 5G technology provide more flexibility and efficiency compared to previous generations. This allowed higher data rates and improved performance in dense urban environments where interference is common [1, 2]. Additionally, the use of numerous subcarrier spacings in 5G technology enables better support for diverse applications with varying requirements, such as enhanced mobile broadband and ultra-reliable low latency communications [3-5]. These numerologies are then assigned to users based on their specific needs and network conditions [6], allowing more efficient and flexible data transmission. By utilizing numerology in 5G downlink, network operators can optimize resource allocation and improve overall network performance. The LTE system utilizes a constant subcarrier spacing of 15 kHz. However, in 5G, it is possible to utilize alternative subcarrier spacing values, such as 15 kHz, 30 kHz, 60 kHz, 120 kHz, 240 kHz, 480 kHz, or 960 kHz [7]. The subcarrier spacing is calculated with the formula:

$$\Delta f = 2\mu \times 15 \quad (1)$$

where  $\mu$  is the numerology index [8], different numerologies can be assigned to users according to their specific requirements and network conditions. Numerologies are used to set different OFDM parameters, such as the Sub-Carrier Spacing (SCS), symbol duration, and Cyclic Prefix (CP) length [9, 10], Table I illustrates the transmission numerologies and their corresponding subcarrier spacing.

The waveform and frame are now more flexible, which lowers latency and boosts reliability [11, 12]. In the 5G frame

structure, the subframe duration of 1 ms is subsequently partitioned into one or more slots, which is determined by the employed numerology index. The higher the numerology index, the higher the number of slots. Figure 1 depicts the frame structure. As a result of using numerology, 5G NR shortens the slot duration down to 125  $\mu$ s [13], the shorter slot duration also improves network latency, making 5G NR ideal for applications requiring real-time communication [14], such as autonomous vehicles or industrial automation. NR 5G channel models are essential for predicting the performance of 5G networks in different environments. These models consider factors, such as path loss, shadowing, and multipath. In addition, they can help in optimization of network planning and deployment strategies. For 5G link-level evaluations, two types of channel models have been established: the Clustered Delay Line (CDL) and the Tapped Delay Line (TDL). Both models feature pre-established profiles labeled as A, B, C, D, and E. Profiles A, B, and C are designed for scenarios with Non-Line-of-Sight (NLoS) conditions, while profiles D and E are specifically for Line-of-Sight (LoS) channels [15-17]. The CDL channel model comprises several independent groups of delayed beams, each one of them contains several path components with the same known delay values but different departure and arrival angles [18, 19]. A TDL added some delay and could also scale the signal if desired [20]. In the TDL, linear finite impulse response is used to represent the channel impulse response, the TDL model assumes that the channel response can be represented as a sum of delayed and attenuated versions of the transmitted signal [21]. The signal between the sender and receiver goes through several steps including precoding at which multiple data streams can be sent at the

same time, it is commonly deployed in MIMO communication systems to enhance the channel gain and minimize interference [22, 23]. Channel estimation is performed at the receiver side. The frequency channel response is estimated so that it can be used in later steps for the equalization of the distorted resource grid [24, 25]. This process is crucial for improving the overall performance of wireless communication systems by minimizing errors and improving signal quality. Additionally, accurate channel estimation allows more efficient use of the available bandwidth and resources. Numerology plays a significant role in determining how resources are allocated and utilized within the Physical Downlink Shared Channel (PDSCH), which is central to the downlink throughput experienced by users. Despite its importance, the impact of numerology on PDSCH throughput has not been extensively studied in the current literature, while other numerology related topics, such as BLER, V2V, and V2X communications have been thoroughly investigated. This study offers a detailed analysis of how varying numerology configurations influence the performance of the PDSCH in most supported transmission bandwidths, which is critical for downlink data transmission. Although many of the existing studies focus on other aspects of 5G performance, this research specifically targets to the PDSCH, which is integral to the end-user experience. It also offers a foundation for optimizing throughput by adjusting numerology indexes.

TABLE I. SUPPORTED TRANSMISSION NUMEROLOGIES

$\mu$	0	1	2	3	4	5	6
$\Delta f$	15	30	60	120	240	480	960

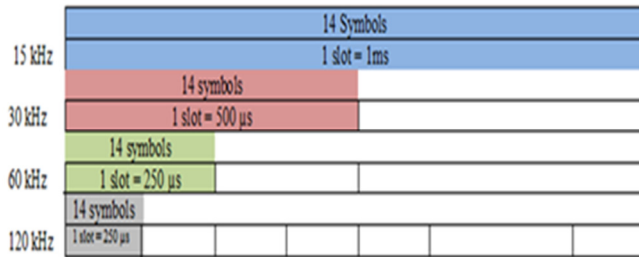


Fig. 1. 5G New Radio (NR) frame structure.

II. METHOD

A comparison was conducted to measure the PDSCH throughput various 5G NR numerologies from 0 to 3 across different channel models (CDL-C, TDL-C) and bandwidths. The throughput is expressed as a function of signal-to-noise ratio. Figure 2 shows every step from the transmitter to receiver. The throughput is calculated using:

$$\text{Throughput}(\text{bps}) = \sum_{j=1}^J (V_{\text{Layers}}^{(j)} \cdot Q_m^{(j)} \cdot f^{(j)} \cdot R_{\text{max}} \cdot \frac{N_{\text{PRB}}^{\text{BW}(j),\mu} \cdot 12}{T_s^\mu} (1 - \text{OH}^{(j)})) \quad (2)$$

where J is the number of aggregated components carrier,  $V_{\text{layers}}^j$  is the number of MIMO layers,  $Q_m^j$  is the modulation order,  $R_{\text{max}}$  is 0.92578125 depending on the type of coding,  $F^j$  is the scaling factor,  $N_{\text{PRB}}^{\text{BW}(j),\mu}$  is the number of physical resource blocks,  $\mu$  is the numerology,  $T_s^\mu$  is the average OFDM duration

symbol for normal cyclic prefix, and  $\text{OH}^{(j)}$  is the overhead. The simulation is implemented using MATLAB. Table II shows the simulation parameters.

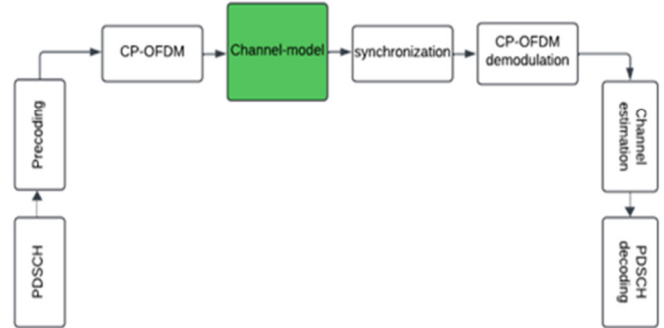


Fig. 2. Block diagram for all the steps between Tx and Rx.

TABLE II. SIMULATION PARAMMETERS

Parameter	value
Number of frames	2
Subcarrier spacing	15, 30, and 60 KHz.
Cyclic prefix	Normal
Number of PDSCH transmission layers	2
Modulation scheme	16 QAM
propagation channel	CDL-C and TDL-C
Number of UE transmit antennas	8
Number of UE receive antennas	2
Precoding technique	Sub-band
Channel estimation	Perfect
Bandwidth	10,20,40 and 50MHz

III. RESULTS AND DISCUSSION

The throughput is evaluated to 10 MHz, 20 MHz, 40 MHz, and 50 MHz for both CDL-C and TDL-C channel models for the numerology index from 0 to 3.

A. 10 MHz

At 10 MHz bandwidth, CDL-C and TDL-C channel models are initially analyzed. The results are portrayed in Figures 3 and 4, respectively.

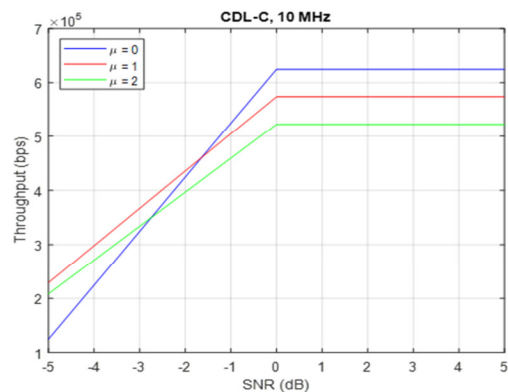


Fig. 3. Throughput for 10 MHz, CDL-C.

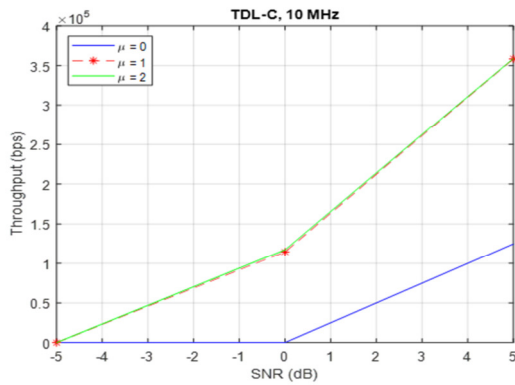


Fig. 4. Throughput for 10 MHz, TDL-C.

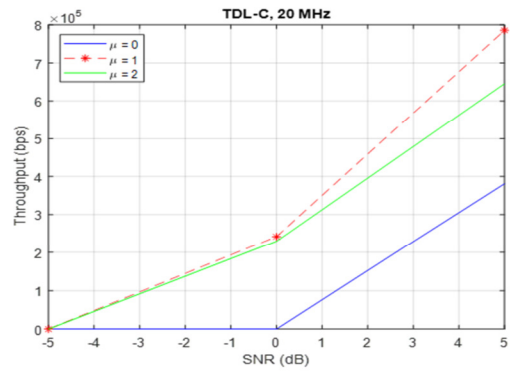


Fig. 6. Throughput for 20 MHz, TDL-C.

The throughput for the CDL-C channel model increases as the numerology value decreases. On the contrary, for the TDL-C channel model, the throughput performance is almost the same for  $\mu = 1$  and  $\mu = 2$ , which is higher than the throughput of  $\mu = 0$ . Another crucial point is that, unlike CDL-C, whose throughput is fixed for SNR values greater than zero, TDL-C experiences an increase in throughput as SNR values rise.

**B. 20 MHz**

By increasing the bandwidth to 20 MHz, the 5G NR numerology has a similar effect on the throughput for the CDL-C channel model to the one detected at 10 MHz. Additionally, for the TDL-C channel model, the throughput values for  $\mu = 1$  and  $\mu = 2$  are approximately the same for low SNR. However, for higher SNR, there is a significant increase in the throughput for  $\mu = 1$  compared to  $\mu = 2$ , as observed in Figures 5 and 6.

**C. 40 MHz**

Figures 7 and 8 evaluate the achievable throughput at 40 MHz for CDL-C and TDL-C, respectively. For the CDL-C, the throughput for  $\mu = 0$  is slightly higher than the throughput of  $\mu = 1$ , followed by  $\mu = 2$  for a higher SNR. For TDL-C at lower SNR levels, as seen in Figure 6, the throughput for  $\mu = 1$  and  $\mu = 2$  is similar. However, as SNR values increase, the difference between the two throughputs becomes more significant.

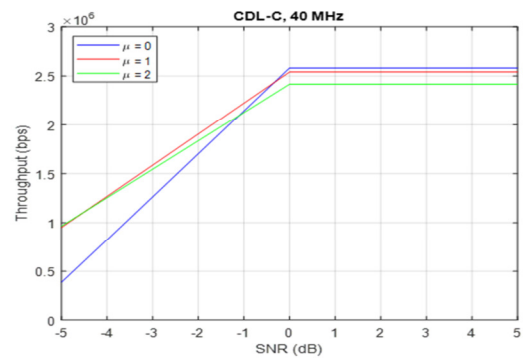


Fig. 7. Throughput for 40 MHz, CDL-C.

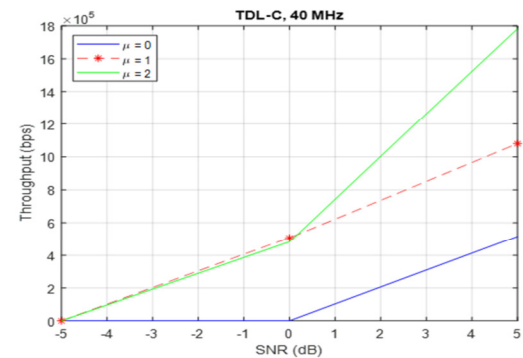


Fig. 8. Throughput for 40 MHz, TDL-C.

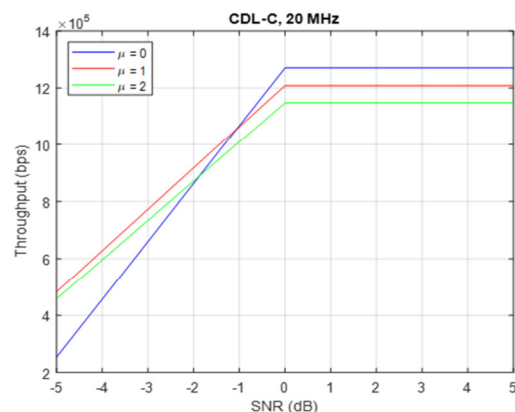


Fig. 5. Throughput for 20 MHz, CDL-C.

**D. 50 MHz**

At 50 MHz bandwidth for the CDL-C, the throughput for  $\mu = 0$  and  $\mu = 1$  is identical, which is higher than the throughput for  $\mu = 2$  at positive values of SNR. On the other hand, the throughput results for  $\mu = 1$  and  $\mu = 2$  of the TDL-C are close to each other, as exhibited in Figures 9 and 10.

The results of the simulation agree well with the findings of [26, 27], considering that the study covers a wide range of bandwidths and is designed to accommodate both indoor and outdoor communication with different channel conditions. For the indoor communication scenario (CDL-C), the throughput drops as the numerology increases, whereas for the outdoor and high speed scenarios (TDL-C), the first numerology has the lowest throughput.

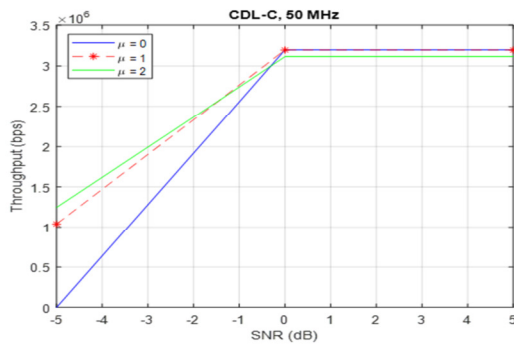


Fig. 9. Throughput for 50 MHz, CDL-C.

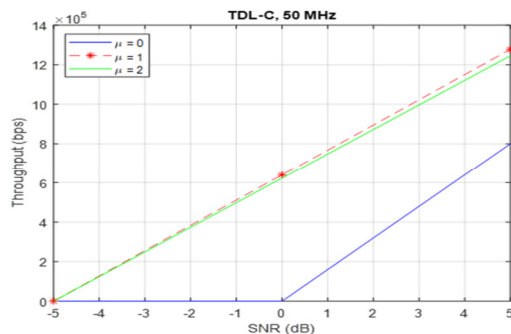


Fig. 10. Throughput for 50 MHz, TDL-C.

#### IV. CONCLUSION

Depending on the channel model, changes in 5G NR numerology have a substantial impact on throughput performance. The simulation results for the CDL-C channel model show that when the numerology is increased, the throughput decreases for all bandwidths except for 50 MHz at which the throughput is the same for  $\mu = 0$  and  $\mu = 1$  for high SNR values. This implies that other considerations, such as implementation complexity, determine whether the first or the second numerology should be used. As the bandwidth increases, the difference in throughputs for numerologies becomes relatively small. For all numerologies, the throughput remains stable when SNR values rise above zero. In contrast to the CDL-C channel model, in the TDL-C, the throughput for  $\mu = 0$  is always less than the throughput for the other numerologies. In some cases, the throughput for  $\mu = 1$  is higher than the throughput for  $\mu = 2$ , and vice versa. This study aims to offer valuable insights for network operators and researchers working towards the refinement of 5G systems. The findings are expected to contribute to the development of network performance, including higher data rates and more efficient use of the available spectrum in the next-generation mobile communications.

#### ACKNOWLEDGMENT

The author extends his appreciation to Prince Sattam bin Abdulaziz University for funding this research work through the project number (PSAU/2023/01/29004).

#### REFERENCES

- [1] A. Narayanan *et al.*, "A First Look at Commercial 5G Performance on Smartphones," in *Proceedings of The Web Conference 2020*, New York, NY, USA, Dec. 2020, pp. 894–905, <https://doi.org/10.1145/3366423.3380169>.
- [2] L. Marijanović, S. Schwarz, and M. Rupp, "Multiplexing Services in 5G and Beyond: Optimal Resource Allocation Based on Mixed Numerology and Mini-Slots," *IEEE Access*, vol. 8, pp. 209537–209555, 2020, <https://doi.org/10.1109/ACCESS.2020.3039352>.
- [3] N. Patriciello, S. Lagen, L. Giupponi, and B. Bojovic, "5G New Radio Numerologies and their Impact on the End-To-End Latency," in *2018 IEEE 23rd International Workshop on Computer Aided Modeling and Design of Communication Links and Networks (CAMAD)*, Sep. 2018, pp. 1–6, <https://doi.org/10.1109/CAMAD.2018.8514979>.
- [4] A. Yazar and H. Arslan, "Reliability enhancement in multi-numerology-based 5G new radio using INI-aware scheduling," *EURASIP Journal on Wireless Communications and Networking*, vol. 2019, no. 1, May 2019, Art. no. 110, <https://doi.org/10.1186/s13638-019-1435-z>.
- [5] M. R. Maganti and K. R. Rao, "Enhancing 5G Core Network Performance through Optimal Network Fragmentation and Resource Allocation," *Engineering, Technology & Applied Science Research*, vol. 14, no. 3, pp. 14588–14593, Jun. 2024, <https://doi.org/10.48084/etasr.7235>.
- [6] S. Khabaz, K. O. Boulila, T. M. Trang Nguyen, G. Pujolle, M. E. Aoun, and P. B. Velloso, "A New Priority and Satisfaction-based Resource Allocation Algorithm with Mixed Numerology for 5G-V2X communications," in *2022 14th IFIP Wireless and Mobile Networking Conference (WMNC)*, Jul. 2022, pp. 85–92, <https://doi.org/10.23919/WMNC56391.2022.9954308>.
- [7] D. Wang, O. Saraci, R. Sattiraju, Q. Zhou, and H. Schotten, "Effect of Variable Physical Numerologies on Link-Level Performance of 5G NR V2X," Dec. 2022, pp. 291–296, <https://doi.org/10.1109/ICCC56324.2022.10065622>.
- [8] X. Cheng, R. Zayani, H. Shaiek, and D. Roviras, "Analysis and Cancellation of Mixed-Numerologies Interference for Massive MIMO-OFDM UL," *IEEE Wireless Communications Letters*, vol. 9, no. 4, pp. 470–474, Apr. 2020, <https://doi.org/10.1109/LWC.2019.2959526>.
- [9] "ts\_138211v170100p.pdf." [https://www.etsi.org/deliver/etsi\\_ts/138200\\_138299/138211/17.01.00\\_60/ts\\_138211v170100p.pdf](https://www.etsi.org/deliver/etsi_ts/138200_138299/138211/17.01.00_60/ts_138211v170100p.pdf).
- [10] A. Yazar and H. Arslan, "Flexible Multi-Numerology Systems for 5G New Radio," *Journal of Mobile Multimedia*, vol. 14, no. 4, pp. 367–394, 2018, <https://doi.org/10.13052/jmm1550-4646.1442>.
- [11] N. Chahboun, A. Bellekhir, J. Zbitou, and Y. Laaziz, "Mutual coupling reduction between antennas array for 5G mobile applications," *Indonesian Journal of Electrical Engineering and Computer Science*, vol. 34, no. 1, pp. 362–369, Apr. 2024, <https://doi.org/10.11591/ijeecs.v34.i1.pp362-369>.
- [12] K. Boutiba, M. Bagaa, and A. Ksentini, "Radio Resource Management in Multi-numerology 5G New Radio featuring Network Slicing," in *ICC 2022 - IEEE International Conference on Communications*, Feb. 2022, pp. 359–364, <https://doi.org/10.1109/ICC45855.2022.9838462>.
- [13] Y. Zhao, M. Wei, C. Hu, and W. Xie, "Latency Analysis and Field Trial for 5G NR," in *2022 IEEE International Symposium on Broadband Multimedia Systems and Broadcasting (BMSB)*, Jun. 2022, pp. 1–5, <https://doi.org/10.1109/BMSB55706.2022.9828792>.
- [14] N. Correia, F. Al-Tam, and J. Rodriguez, "Optimization of Mixed Numerology Profiles for 5G Wireless Communication Scenarios," *Sensors*, vol. 21, no. 4, Jan. 2021, Art. no. 1494, <https://doi.org/10.3390/s21041494>.
- [15] F. Altheeb, I. Elshafiey, M. Altamimi, and A.-F. A. Sheta, "Customized Millimeter Wave Channel Model for Enhancement of Next-Generation UAV-Aided Internet of Things Networks," *Sensors*, vol. 24, no. 5, Jan. 2024, Art. no. 1528, <https://doi.org/10.3390/s24051528>.
- [16] A. M. Pessoa, B. Sokal, C. F. M. E. Silva, T. F. Maciel, A. L. F. De Almeida, and F. R. P. Cavalcanti, "A CDL-Based Channel Model With Dual-Polarized Antennas for 5G MIMO Systems in Rural Remote Areas," *IEEE Access*, vol. 8, pp. 163366–163379, 2020, <https://doi.org/10.1109/ACCESS.2020.3020538>.

- [17] D. A. Urquiza Villalonga, H. OdetAlla, M. J. Fernández-Getino García, and A. Flizikowski, "Spectral Efficiency of Precoded 5G-NR in Single and Multi-User Scenarios under Imperfect Channel Knowledge: A Comprehensive Guide for Implementation," *Electronics*, vol. 11, no. 24, Jan. 2022, Art. no. 4237, <https://doi.org/10.3390/electronics11244237>.
- [18] J. Baghous, "5G system throughput performance evaluation using Massive-MIMO technology with Cluster Delay Line channel model and non-line of sight scenarios," *Infocommunications journal*, vol. 13, pp. 40–45, Jan. 2021, <https://doi.org/10.36244/ICJ.2021.2.6>.
- [19] N. Kumari, Reemakshi Rajput, and S. Sharma, "CDL Channel Model: Revolutionizing Wireless Communication," Aug. 2023, <https://doi.org/10.5281/ZENODO.8216719>.
- [20] S. Jana, A. K. Mishra, and M. Z. A. Khan, "Sensing the Environment with 5G Scattered Signals (5G-CommSense): A Feasibility Analysis," in *2023 IEEE Applied Sensing Conference (APSCON)*, Jan. 2023, pp. 1–3, <https://doi.org/10.1109/APSCON56343.2023.10101090>.
- [21] C.-X. Wang, J. Bian, J. Sun, W. Zhang, and M. Zhang, "A Survey of 5G Channel Measurements and Models," *IEEE Communications Surveys & Tutorials*, vol. 20, no. 4, pp. 3142–3168, 2018, <https://doi.org/10.1109/COMST.2018.2862141>.
- [22] M. A. Albreem, A. H. A. Habbash, A. M. Abu-Hudrouss, and S. S. Ikki, "Overview of Precoding Techniques for Massive MIMO," *IEEE Access*, vol. 9, pp. 60764–60801, 2021, <https://doi.org/10.1109/ACCESS.2021.3073325>.
- [23] P. Nguyen T. H., T.-N. To, D. Tran-Thi, and Q. Le-Trung, "5G Channel Estimation Based on Whale Optimization Algorithm," *Wireless Communications and Mobile Computing*, vol. 2023, no. 1, 2023, Art. no. 5800673, <https://doi.org/10.1155/2023/5800673>.
- [24] P. M. Aviles, D. Lloria, J. A. Belloch, S. Roger, A. Lindoso, and M. Cobos, "Performance analysis of a millimeter wave MIMO channel estimation method in an embedded multi-core processor," *The Journal of Supercomputing*, vol. 78, no. 12, pp. 14756–14767, Aug. 2022, <https://doi.org/10.1007/s11227-022-04479-3>.
- [25] W. Hussein, N. K. Noordin, K. Audah, M. F. B. A. Rasid, A. B. Ismail, and A. Flah, "Cascaded and Separate Channel Estimation based on CNN for RIS-MIMO Systems," *Engineering, Technology & Applied Science Research*, vol. 14, no. 3, pp. 14768–14774, Jun. 2024, <https://doi.org/10.48084/etasr.7499>.
- [26] M. Ali, "Performance Analysis of Physical Downlink Shared Channels for 5G New Radio," Aug. 2019.
- [27] S. Khabaz, K. O. Boulila, T. M. Trang Nguyen, G. Pujolle, M. El Aoun, and P. B. Velloso, "A Comprehensive Study of the Impact of 5G Numerologies on V2X Communications," in *2022 13th International Conference on Network of the Future (NoF)*, Jul. 2022, pp. 1–9, <https://doi.org/10.1109/NoF55974.2022.9942567>.